A semi-discretization approach to buckling behavior of thin-walled members

Andreassen, Michael Joachim; Jönsson, Jeppe

Published in:
Proceedings of the 7th European conference on steel and composite structures (EUROSTEEL 2014)

Publication date:
2014

EUROSTEEL 2014, September 10-12, 2014, Naples, Italy

A SEMI-DISCRETIZATION APPROACH TO BUCKLING BEHAVIOR OF THIN-WALLED MEMBERS

Michael Joachim Andreassen, Jeppe Jönsson

Technical University of Denmark, Department of Civil Engineering
Brovej building 118, DK-2800 Kgs. Lyngby, Denmark
mican@byg.dtu.dk, jej@byg.dtu.dk

INTRODUCTION

The classic stability analysis of thin-walled columns is based on ‘‘in-plane rigid’’ cross-section displacement modes corresponding to: Uniform axial extension, major axis bending, minor axis bending and torsion with related warping. An important feature missing here is the deformation of the cross section, which undergoes in-plane deformations by local and distortional modes.
This paper deals with a novel method based on solution of the differential equations of GBT obtained through semi-discretization and application of beam constraints.
In contrast to the traditional GBT formulations, this novel approach finds the exact modes shapes and amplitude solutions of the reduced order GBT equations related to the discretized cross section. For a more elaborate description see the companion papers, [1-5].
In this conference paper the novel approach is extended by including the initial stress terms. This leads to a modified set of coupled homogeneous differential equations of GBT with initial stress for identification of distortional buckling modes. In this paper we seek simple instability solutions using these GBT initial stress equations for the classical simply supported columns with constrained transverse displacements at the end sections and a constant axial initial stress. Based on the known boundary conditions the reduced order differential equations are solved by introducing the relevant trigonometric solution function and solving the related eigenvalue problem. This directly gives us the cross-section buckling mode shape and the eigenvalue corresponding to the bifurcation load factor.
An illustrative example is given including development of classic buckling curves and comparison of results with finite element results found using Abaqus as well as with FSM and conventional GBT results found using the freely available software packages CUFSM [6] and GBTUL [7].

1 BEAM KINEMATICS OF A SINGLE MODE

A prismatic thin-walled beam is considered and described in a global Cartesian (x, y, z) coordinate system as shown in *Fig 1*.

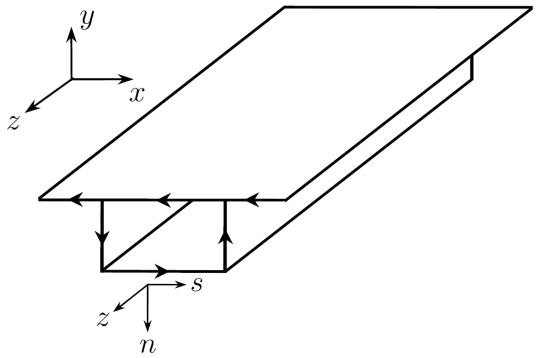

Fig. 1. Global and local Cartesian reference frames.

In the associated local coordinate system (z, n, s) the displacements u_n, u_s and u_z of a material point are defined as,

$$u_n(s,z) = \mathrm{w}_n(s)\psi(z) \tag{1}$$

$$u_s(n,s,z) = \left(\mathrm{w}_s(s) - n\mathrm{w}_{n,s}(s)\right)\psi(z) \tag{2}$$

$$u_z(n,s,z) = -\left(\Omega(s) + n\mathrm{w}_n(s)\right)\psi'(z) \tag{3}$$

Here $\mathrm{w_s}$(s) and $\mathrm{w_n}$(s) describes the local displacements of the centreline, z is the function which describes the variation along the beam and, s describes the axial (warping) displacement mode. The local components are shown in *Fig. 2*.

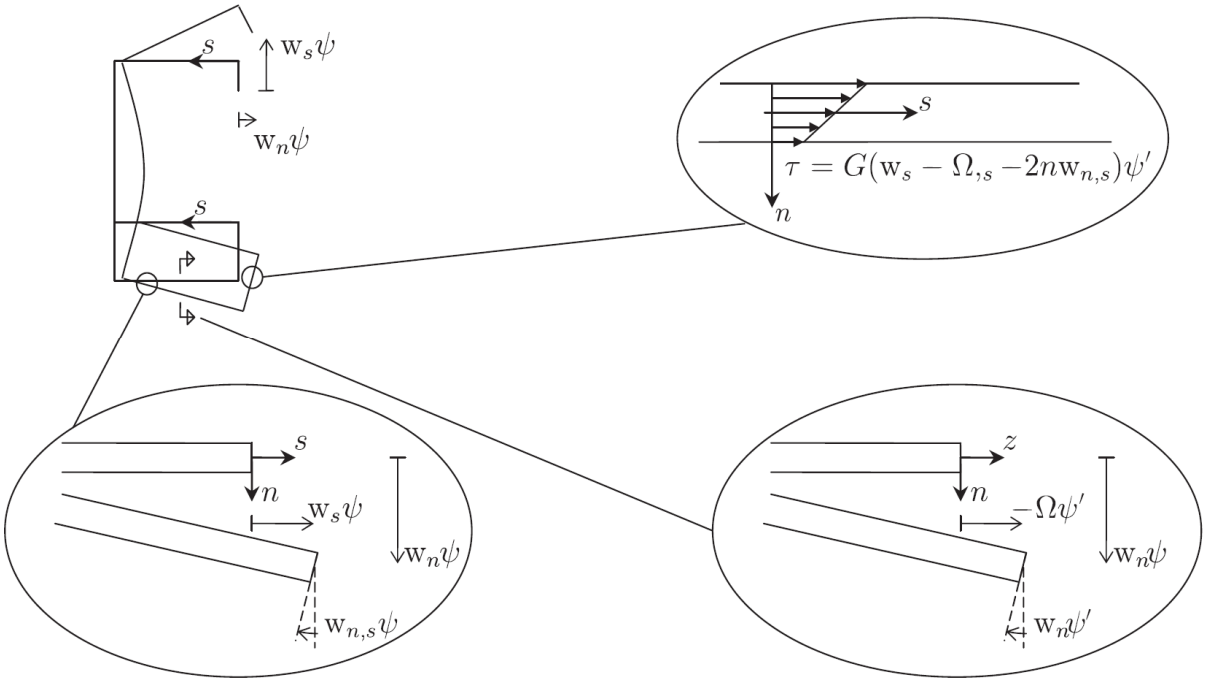

Fig. 2. Local components of displacements and assumed shear stresses.

The notation indicates the two dimensions of the cross section plane and the single dimension associated with the variation along the beam. The strain components associated with the given displacements in *Eq.* (1)-(3) are found as,

$$\varepsilon_z = -(\Omega + n\mathrm{w}_n)\psi'' \tag{4}$$

$$\varepsilon_s = (\mathrm{w}_{s,s} - n\mathrm{w}_{n,ss})\psi \tag{5}$$

$$\gamma_{zs} = (\mathrm{w}_s - \Omega_{,s} - 2n\mathrm{w}_{n,s})\psi' \tag{6}$$

For a greater explanation and description see the related papers [1-5].

2 ENERGY POTENTIAL OF A SINGLE MODE AND INITIAL STRESS

The internal energy potential is presented in paper [5] and only the factored initial stress contribution of a single mode to the potential energy will be presented here. The factored initial stress contribution takes the following form after introduction of straight cross-sectional wall elements, displacement derivatives and integration through the thickness:

$$\Pi_0 = \frac{1}{2}\int_0^L \left[\sum_{el}\int_0^{b_{el}} \lambda\sigma^0 \left\{ t(\mathrm{w}_n\psi')^2 + t(\mathrm{w}_s\psi')^2 + \frac{1}{12}t^3(\mathrm{w}_{n,s}\psi')^2 \right\} ds\right] dz \tag{7}$$

The introduction of the displacement interpolations leads to the definition of the geometric stiffness matrix for a single wall element. Transforming from local to global components using a standard formal finite element transformation and assembly matrix we get the global geometrical stiffness matrix, and thus equation (7) in reduced form can be rewritten as

$$\Pi_0 = \frac{1}{2}\int_0^L \left\{ \begin{bmatrix} \psi \mathbf{v}_w^T & \psi \mathbf{v}_\Omega^T \end{bmatrix}' \begin{bmatrix} \lambda \mathbf{K}^0 & \mathbf{0} \\ \mathbf{0} & \mathbf{0} \end{bmatrix} \begin{bmatrix} \psi \mathbf{v}_w \\ \psi \mathbf{v}_\Omega \end{bmatrix}' \right\} dz \tag{8}$$

which is the contribution to the potential energy from the factored initial stress.

To obtain a formulation resembling a generalization of Vlasov beam theory including distortion, we have to perform the following main steps:

- In step I the shear constraint equations that bind axial and transverse modes together are introduced. In this process the singularity in the shear stiffness matrix related to pure axial extension is eliminated.
- In step II two eigenmodes corresponding to transverse translation of the cross section are identified and eliminated. Also the transverse displacement field is constrained, so that transverse normal strains in the middle surface of the cross section are not allowed, i.e. $w_{s,s} = 0$ is enforced, see *Eq.* (5). Furthermore the order of the coupled fourth order differential equations is reduced by a transformation into twice as many second order differential equations by using a state vector.

This reveals the following final formal second order matrix differential equation of double size:

$$\begin{bmatrix} \tilde{\mathbf{K}}^s & \mathbf{0} \\ \mathbf{0} & -\tilde{\mathbf{K}}^\sigma \end{bmatrix} \begin{bmatrix} \tilde{\mathbf{v}}_w \psi \\ \tilde{\mathbf{v}}_w \psi'' \end{bmatrix} - \left(\begin{bmatrix} \tilde{\mathbf{K}}^\tau & -\tilde{\mathbf{K}}^\sigma \\ -\tilde{\mathbf{K}}^\sigma & \mathbf{0} \end{bmatrix} + \lambda \begin{bmatrix} \tilde{\mathbf{K}}^0 & \mathbf{0} \\ \mathbf{0} & \mathbf{0} \end{bmatrix} \right) \begin{bmatrix} \tilde{\mathbf{v}}_w \psi \\ \tilde{\mathbf{v}}_w \psi'' \end{bmatrix}'' = \begin{bmatrix} \mathbf{0} \\ \mathbf{0} \end{bmatrix} \tag{9}$$

By substituting A, B, C and u_s for the respective matrices and vector the equation takes the following form:

$$\mathbf{A}\mathbf{u}_S - [\mathbf{B} + \lambda \mathbf{C}]\mathbf{u}_S'' = \mathbf{0} \tag{10}$$

This is the set of differential equations to which we want to find solutions.

3 DISTORTIONAL INITIAL STRESS EIGENVALUE PROBLEM

In order to satisfy suitable simple boundary conditions it is assumed that the solution is of a simple trigonometric form here chosen as $\psi(z) = \sin \mu z$, where $\mu = n\pi/L$ in which n is equal to the number of buckles, i.e. half-wavelengths. This solution satisfies boundary conditions corresponding to simple supports with restrained transverse cross-section displacements at z = 0 and z = L. Inserting this postulated solution in *Eq.* (10) leads to the following generalized linear symmetric matrix eigenvalue problem, in which the eigenvalues, λ, correspond to the buckling factor and the eigenvectors are the distortional state space buckling modes:

$$\left[\mathbf{A} + \left(\frac{n\pi}{L}\right)^2 \mathbf{B} \right] \mathbf{v}_S + \lambda \left(\frac{n\pi}{L}\right)^2 \mathbf{C}\mathbf{v}_S = \mathbf{0} \tag{11}$$

Eliminating the second half of vector $\mathbf{v_s}$ corresponding to $\tilde{\mathbf{v}}_w \psi''$ in equation (11) leads to the following final generalized linear symmetric matrix eigenvalue problem:

$$[\mathbf{K} + \lambda \mathbf{G}]\tilde{\mathbf{v}}_w = \mathbf{0} \tag{12}$$

From the results of this eigenvalue problem we know at which load (λ) the corresponding mode has a homogeneous solution function which is sinusoidal with a number of half-waves corresponding to n, leading to conventional half-wavelength buckling curves or so called cross-section signature curves as given in the next chapter.

4 EXAMPLE

In this section the ability of the developed GBT approach to produce buckling curves and predict buckling is shown. The example considers a simply supported lipped channel column in uniform compression. The end sections are constrained against transverse displacements, but otherwise free to warp and thus also to rotate. The chosen in-plane geometry and the discretization are shown in

Fig. 3. The accuracy of the results is assessed by comparison to results obtained by the use of the commercial FE program Abaqus. For an elaborate description of the Abaqus FE model see paper [2]. Solving the GBT initial stress eigenvalue problem given in *Eq.* (11) with n=1 for half-wave

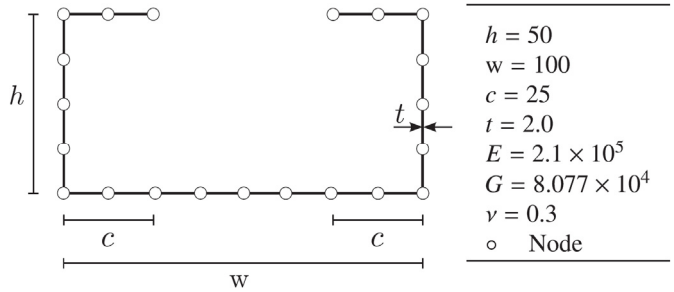

Fig. 3. Geometry, discretization and parameter values of a lipped channel column.

lengths L varying from10 mm to 3000 mm (logarithmical spaced) allows the development of the signature curve as shown in *Fig. 4*. The buckling curves shown in the figure correspond to the four

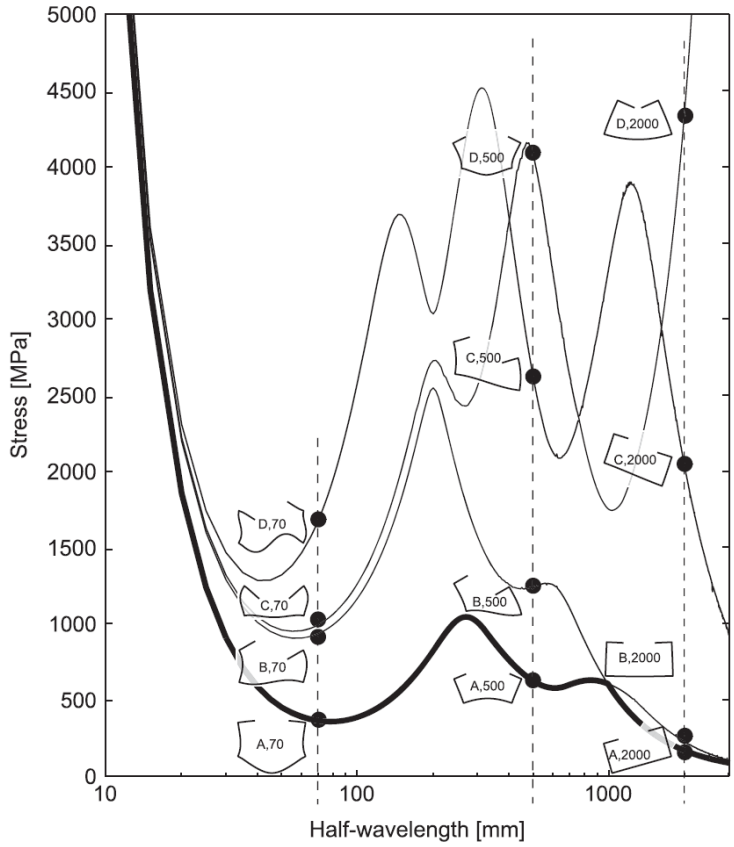

Fig. 4. Buckling signature curve corresponding to the lowest four modes with a single half-wave buckle, n=1.

lowest buckling modes with a single half-wave buckle, n=1. For three different half-wavelengths the transverse buckling mode shape has been depicted in the figure. The chosen half-wavelengths correspond to the dashed lines at 70mm, 500 mm and 2000 mm, respectively.

From the figure it is seen that each developing mode represents its own curve placed in a hierarchical order according to the stress level. However, the curves are able to change place in the hierarchy at a certain column length. This phenomenon can for example be seen for buckling mode 1 and 2 (two lowest ranking graphs) at a column length of approximately 1000 mm. The signature curve, shown bold, is achieved as the very lowest of the buckling curves. For this curve a short column lengths correspond to local buckling, while for increasing column lengths it corresponds to distortional buckling and finally for large column lengths it corresponds to global buckling. The signature curve is similar to the finite strip buckling curve obtained by Hancock [8]. As mentioned *Fig. 4* is for a half-wavenumber n=1. As the buckling loads also depend on the number of n half waves in the buckled shapes, this means that points lower than the signature curve can exist for a

greater number of buckles, n>1. To show this phenomenon the signature curve has been created for a varying number of n as shown in *Fig. 5*.

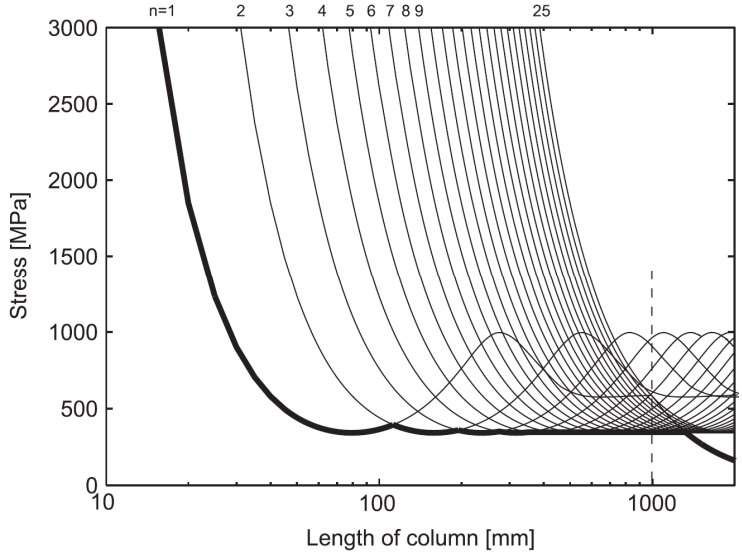

Fig. 5. Buckling stress versus column length for the lipped channel section in compression.

This means that the bold curve shown in *Fig. 5* represents the absolute lowest curve for the buckling stress versus column length. However, to illustrate the multitude of buckling modes for each column length, let us look at a column length of L=1000 mm. In *Fig. 5* this length is represented by the vertical dashed line. For this length we can find the buckling modes m=1, 2, 3.. ordered from lowest to highest critical stress, each having a different number of half waves n. In *Table 1* the buckling stresses of FE analysis using Abaqus versus the presented GBT method, conventional GBT using GBTUL and FSM using CUFSM are compared.

Table. 1: Comparison of buckling stresses for FE analysis versus the presented GBT method, GBTUL and CUFSM, respectively. The comparisons are related to the vertical dashed m-line in *Fig. 5*.

m	Nr. of half waves n	Abaqus [MPa]	GBT [MPa]	Diff. %	GBTUL [MPa]	Diff. %	CUFSM [MPa]	Diff. %
1	13	404	350	13.4	412	2.0	412	2.0
20	1	580	590	1.7	589	1.6	581	0.2
24	3	903	918	1.7	933	3.3	906	0.3

The comparison is performed for suitable mode numbers (m-values) and the associated relevant buckling modes which shows the local buckling mode corresponding to the lowest critical stress (m=1), the global beam buckling mode (m=20) and a distortional mode shape (m=24), respectively. The three values of m have been chosen to show the spectrum of modes represented at the given beam length. From *Table 1* it is seen that for a column length of 1000 mm buckling will occur as local buckling consisting of thirteen sine half waves and have an associated buckling stress of 350MPa. Furthermore it is seen that the buckling mode shape for mode m=20 is global column buckling with a single buckle, n=1, at a stress level of 590 MPa and finally for m=24 distortional column buckling occurs at a stress level of 918 MPa. Comparing the GBT buckling stresses with Abaqus we obtain a deviation of 13.4% for local plate buckling, 1.7% for global buckling and 1.7% for distortional buckling. Hereby it is seen that good results are obtained for global and distortional buckling, while a rather large deviation is obtained for local buckling. The GBTUL results which are based on the classic GBT theory shows a deviation of 2.0% for local plate buckling, 1.6% for global buckling and 3.3% for distortional buckling. In contrast to these beam theory results, *Table 1* also shows results obtained from the CUFSM program which is based on a plate theory. Here we obtain a deviation of 2.0% for local plate buckling, 0.2% for global buckling and 0.3% for distortional buckling, showing that good results are obtained in all cases. From the deviations it is obvious that GBT and GBTUL are based on beam theories while CUFSM is based on plate theory.

The rather large deviation of 13.4% for the GBT results compared with the deviation of 2.0% obtained with GBTUL, can to a certain extent be explained by the very simple constitutive relations used in the current GBT formulation. Making a calculation in Abaqus with similar very simple non-coupling constitutive relations the deviations obtained now corresponds to (350MPa) 0.0%, (582MPa) 1.4% and (888MPa) 3.4%, respectively. Hereby good matches between the two approaches are obtained, however, also difference in the modelling of the boundary conditions can affect the results. Thus demonstrating that this new developed GBT approach provides reasonably accurate results with a very small computational cost, making it an alternative to the traditional and time consuming FE calculations and the other available methods. However, the constitutive relations should be modified to achieve a higher accuracy for local plate buckling.

5 CONCLUSION

This conference paper presented the extension of the novel GBT approach developed by the authors in [1-5] to include the geometrical stiffness terms which are needed for column buckling analysis. The distortional differential equations developed in paper [1-5] are extended to a formulation including geometrical stiffness terms by using the initial stress approach to formulate the instability problem. The derived GBT differential equations with initial stress have been solved
as an eigenvalue problem leading to a number of buckling modes and associated buckling stresses for simply supported columns in compression. An illustrative example has been given dealing with a lipped channel column section.
In order to illustrate the application and validity of the approach the results have been compared with FE results obtained using the commercial program Abaqus as well as with FSM and conventional GBT results found using the freely available software packages CUFSM and GBTUL, respectively. Reasonable matches are obtained confirming that this new developed GBT approach including geometrical stiffness terms provides reasonable results with a very small computational cost making it an alternative to the traditional and time consuming FE calculations and the other available methods. However the constitutive relations may have to be modified in order to achieve higher accuracy for local plate buckling.

REFERENCES

[1] Andreassen M.J., 2012. “Distortional mechanics of thin-walled structural elements”, *Ph. D. thesis*, DTU Civil Engineering, Department of Civil Engineering, Technical University of Denmark.

[2] Andreassen M.J., Jönsson J., 2012. “Distortional buckling modes of semi-discretized thin-walled columns”. *Thin-Walled Structures*, Vol. 51, pp. 53-63.

[3] Andreassen M.J., Jönsson J., 2012. “Distortional solutions for loaded semi-discretized thin-walled beams”. *Thin-Walled Structures*, Vol. 50, pp. 116-127.

[4] Andreassen M.J., Jönsson J., 2013. “A distortional semi-discretized thin-walled beam element”. *Thin-Walled Structures*, Vol. 62, pp. 142-157.

[5] Jönsson J., Andreassen M.J., 2011. “Distortional eigenmodes and homogeneous solutions of semi-discretized thin-walled beams”, *Thin-Walled Structures*, Vol. 49, pp. 691-707.

[6] Li Z., Schafer B.W., 2010. “Buckling analysis of cold-formed steel members with general boundary conditions using CUFSM: conventional and constrained finite strip methods”, *Proceedings of the 20th international special conference on cold-formed steel structures*, 3 November – 4 November, 2010, St. Louis, Missouri, U.S.A, pp. 17-31.

[7] Bebiano R., Pina P., Silvestre N., Camotim D., 2008. “GBTUL—buckling and vibration analysis of thin-walled members”. *DECivil/IST, Technical University of Lisbon,* (http://www.civil.ist.utl.pt/gbt).

[8] Hancock G.J., 1985. “Distortional buckling of steel storage rack column”. *Journal of Structural Engineering,* Vol. 12, pp. 111.